Angewandte Chemie
Eine Zeitschrift der Gesellschaft Deutscher Chemiker

Supporting Information

69451 Weinheim, Germany

Formation of Vesicular Structures via the Self-Asssembly of Flexible Zwitterions in DMSO

Carsten Schmuck,*[1] Thomas Rehm[1], Katja Klein,[2] Franziska Gröhn[2]

[1]*University of Würzburg, Institute of Organic Chemistry, Am Hubland, 97074 Würzburg, Germany*

[2]*Max Planck Institute for Polymer Research, Ackermannweg 10, 55128 Mainz, Germany.*

General Information: All solvents were dried and distilled under nitrogen before use. All other reagents were used as obtained from either Aldrich or Fluka. Reactions were monitored by TLC on silica gel plates (*Machery-Nagel* POLYGRAM SIL G/UV254). Visualization of the spots was carried out by fluorescence quenching with 254 nm UV light. All melting points were measured with a *Büchi* SMP-20 apparatus according to *Dr. Tottoli* with open end glas capillary tubes. The melting points are not corrected. The NMR spectra were recorded at room temperature with a *Bruker* AV 400 NMR spectrometer. The ^{1}H NMR spectra were recorded at 400 MHz, the ^{13}C NMR spectra at 100 MHz. The chemical shifts are relative to the signals of the used solvents: DMSO-d_6 (d_{1H} = 2.50 and d_{13C} = 39.52), $CDCl_3$ (d_{1H} = 7.26 and d_{13C} = 77.16). The apparent coupling constants are given in Hertz. The description of the fine structure means: s = singulett, br.s = broad singulett, d = dublett, t = triplett, q = quartett, m = multiplett, dt = dublett of triplett. All IR spectra were measured as KBr pellets on a *Jasco* FT-IR 410 spectrophotometer. The maxima are classified in three intensities: s (strong), m (middle), w (weak) and are reported in cm^{-1}. All mass spectra were recorded with a MicroTOF focus spectromter (*Bruker Daltonics*).

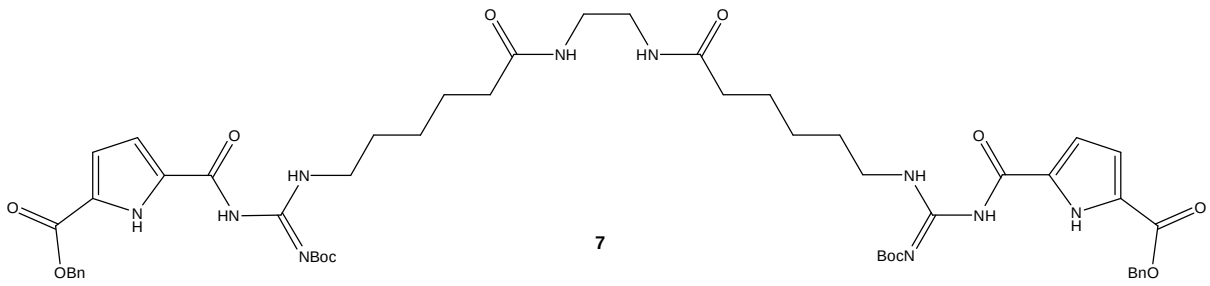

7

A solution of **5**[1] (3.18 g, 6.34 mmol, 2 eq) and PyBOP (3.3 g, 6.34 mmol, 2 eq) in DMF (80 ml) and *N*-Methylmorpholine (8 ml) was stirred for one hour at room temperature. After the addition of 1,2-Diamino ethane **6** (212 µl, 3.17 mmol, 1 eq) the reaction mixture was stirred for 24 hours at room temperature. The slightly yellow solution was poured into water (300 ml) and extracted with diethylether (3 x 200 ml). The organic phase was dried with magnesium sulphate and concentrated *in vacuo*. The crude product was purified by column chromatography (SiO_2, ethylacetat/cyclohexane/isopropanol = 7/2/1 + 1 % triethylamine). For further purification the resulting oil was lyophilised from water/methanol (v/v 9/1) yielding **7** as a white solid (1.40 g, 1.37 mmol, 43 %).

mp: 75 °C; R_f = 0.36 (SiO_2, ethylacetat/cyclohexane/isopropanol = 7/2/1 + 1 % triethylamine); ^{1}H-NMR (400 MHz, DMSO-d_6): d = 1.48 (s, 18H, ^{t}Bu), 1.50-1.57 (m, 12H, CH_2), 2.04 (t, 4H, ^{3}J = 7.32 Hz CH_2CONH), 3.05-3.06 (m, 4H, CH_2), 3.49 (dt, 4H, $^{3}J_{CHCH}$ = 6.68 Hz, $^{3}J_{CHNH}$ = 6.44 Hz, NHCH_2CH$_2$), 5.29 (s, 4H, benzyl-CH_2), 6.76-6.79 (m, 2H, pyrrole-C*H*), 6.82-6.83 (m, 2H, pyrrole-C*H*) 7.31-7.46 (m, 10H, aryl-C*H*), 7.74 (br.s, 2H, CON*H*CH$_2$), 8.55 (t, 2H, $^{3}J_{NHCH}$ = 5.8 Hz, N*H*CH$_2$CH$_2$), 11.81 (br.s, 2H, N*H*), 12.34 (br.s, 2H, N*H*); ^{13}C-NMR (100 MHz, DMSO-d_6): d = 24.9 (*C*H$_2$), 25.9 (*C*H$_2$), 27.6 (*C*H$_3$, ^{t}Bu), 28.5

[1] C. Schmuck, T. Rehm, F. Gröhn, K. Klein, F. Reinhold *J. Am. Chem. Soc.* **2006**, *128*, 1430-1431.

(CH_2), 35.3 (CH_2), 38.3 (CH_2), 40.7 (CH_2), 65.4 (benzyl-CH_2), 83.1 (C_q, ^{t}Bu), 114.2 (pyrrole-CH), 115.7 (pyrrole-CH), 124.8 (C_q), 127.9, 128.0, 128.4 (aryl-CH), 135.5 (C_q), 136.3 (C_q), 152.1 (C_q), 155.5 (C_q), 159.8 (C_q), 169.9 (C_q), 172.1 (C_q); FT IR (KBr) $\tilde{n}$ [cm^{-1}] = 3319 [m], 3034 [w], 2981 [w], 2935 [m], 2860 [w], 1718 [s], 1619 [s], 1584 [s], 1545 [s], 1367 [s], 1276 [s], 779 [w]; HR-MS (ESI pos.) m/z = 1025.510 (calculated for $C_{52}H_{68}N_{10}O_{12}$ + H^+: 1025.5095).

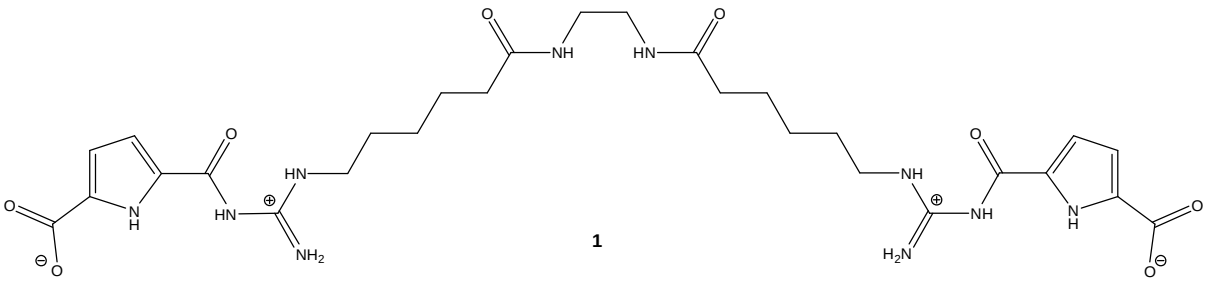

1

A solution of **7** (1.4 g, 1.37 mmol, 1 eq) and palladium on activated charcoal (140 mg) in tetrahydrofuran was stirred for four hours under hydrogen atmosphere. The reaction was controlled via tlc (ethylacetat/cyclohexane/isopropanol = 7/2/1 + 1 % triethylamine). After that the reaction mixture was filtered over a celite pad and washed several times with ethylacetate. The solvent was evaporated and the resulting oil was dried in high vacuum. After the addition of trifluoracetic acid (3 ml) the reaction mixture was stirred for two hours at room temperature. After that the remaining trifluoracetic acid was removed in high vacuum. The resulting oil was dissolved in water and 0.5 N sodium hydroxide solution was added until a white solid precipitated (pH ~ 5 to 6). The crude product was filtered, washed several times with water and lyophilised from water resulting **1** as a white powder (870 mg, 1.35 mmol, 99 %). For further purification **1** (120 mg) was diluted in water/dioxan (40 ml, 1/1, v/v) and refluxed for one hour. The slightly white suspension was filtered and washed several times with pure water and diethylether. The resulting white solid (116 mg) was dried in high vacuum. The picrate salt of **1** was produced by suspending some milligrams of **1** in methanol (5 ml) with a few drops of 1 N sodium hydroxide solution. Addition of aqueous picric acid yielded the yellow picrate salt, which was filtered and dried in high vacuum.

1 (picrate salt): mp: > 240 °C; ^{1}H-NMR (400 MHz, DMSO-d_6): d = 1.23-1.33 (m, 4H, CH_2), 1.48-1.58 (m, 8H, CH_2), 2.06 (t, 4H, ^{3}J = 7.48 Hz CH_2CONH), 3.06-3.07 (m, 4H, CH_2), 3.28-3.31 (m, 4H, CH_2), 6.85-6.87 (m, 2H, pyrrole-CH), 7.01-7.02 (m, 2H, pyrrole-CH), 7.81 (br.s, 2H, CONHCH_2), 8.58 (s, 4H, picrate-CH), 8.77 (br.s., 2H, NHCH_2), 10.75 (br.s, 2H, NH), 12.67 (br.s, 2H, pyrrole-NH), 13.10 (br.s, 2H, COOH); The guanidinio-NHs (4H) are superposed by picrate-CHs and amide-NHs. ^{13}C-NMR (100 MHz, DMSO-d_6): d = 24.7 (CH_2), 25.7 (CH_2), 27.7 (CH_2), 35.2 (CH_2), 38.3 (CH_2), 41.1 (CH_2), 115.2 (pyrrole-CH), 115.4 (pyrrole-CH), 124.1 (C_q), 125. 1 (picrate-CH), 127.1 (C_q), 129.2 (C_q), 141.8 (C_q), 152.9 (C_q), 160.8 (C_q), 161.2 (C_q), 172.1 (C_q); FT IR (KBr) $\tilde{n}$ [cm^{-1}] = 3261 [w], 3187 [m], 31 [w], 2992 [w], 2939 [m], 2858 [w], 1717 [m], 1654 [s], 1557 [m], 1491 [m], 1355 [s], 1324 [s]; HR-MS (ESI pos.) m/z = 645.311 (calculated for $C_{28}H_{40}N_{10}O_8$ + H^+: 645.3108).

NMR Dilution studies:

Solutions of **1** with varying concentrations (from 0.5 to 50 mM) were obtained by diluting aliquots of concentrated stock solutions in DMSO-d_6 to a total volume of 600 µl. The chemical shifts were recorded for each sample relative to the deuterated solvent.

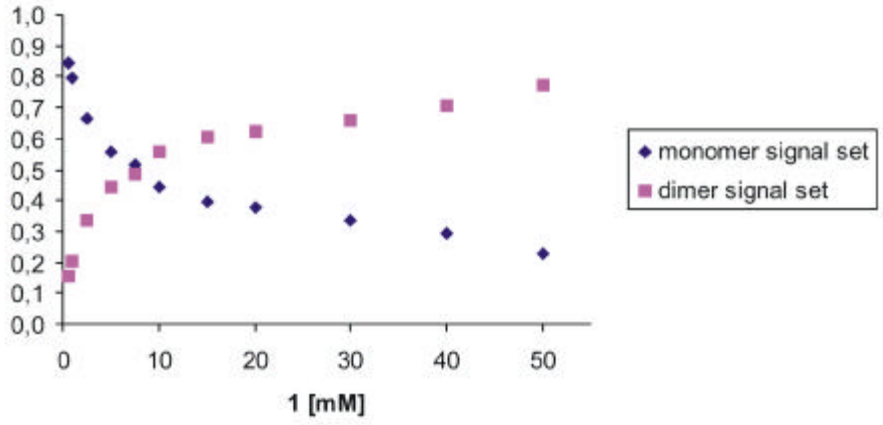

Figure S1. Intensity of the pyrrole-NH nmr signal of **1** for both signal sets depending on varying concentration.

DOSY NMR experiments:

Solutions of **1** (1 and 30 mM), **7** (1 mM) were obtained by diluting aliquots of concentrated stock solutions in DMSO-d_6 to a total volume of 600 µl. TMS was used as internal reference. For each sample the chemical shifts and diffusion coefficients were recorded on a *Bruker* DMX 600 spectrometer equipped with a gradient unit and a conventional 5 mm broadband (^{15}N-^{31}P)/^{1}H probe with automatic tune/match accessory and z axis gradient coil capable of producing pulsed magnetic field gradients in z direction of 52 G cm^{-1}. The longitudinal eddy current delay sequence with bipolar gradient pulse pairs for diffusion (BPP-LED)[2] and additional sinusoidal spoil gradients after the second and fourth 90° pulses was used with the following acquisition parameters: duration d of a bipolar gradient pulse: between 5.0 ms and 8.0 ms, diffusion time ? : 50 ms, spoiler gradient duration: 5.0 ms, spoiler gradient strengths: 17.13 and 13.17 % of maximum gradient strength in 32 linear steps. Signal averaging from 16 to 288 scans per increment as required for adequate signal-to-noise ratio. Data were acquired and processed using the software XWIN-NMR 3.5, patch level 6. For the determination of the diffusion coefficients *D* only nmr signals of non-exchanging protons were used.

1 (1 mM, *T* = 299.1 K) monomer signal

d [ppm]	log *D*	
7,723	-9,939	
6,864	-9,935	
6,531	-9,942	
3,321	-9,065	H_2O
3,262	-9,925	
3,106	-9,945	
3,064	-10,003	
2,501	-9,168	DMSO
2,063	-9,953	
1,591	-9,956	
1,533	-9,955	
1,311	-9,938	
0,000	-9,203	TMS

1 (30 mM, *T* = 299.1 K) dimer signal

[2] Wu, D.; Chen, A.; Johnson, C. S. Jr. *J. Magn. Reson. A* **1995**, *115*, 260-264.

d [ppm]	log *D*	
7,844	-10,185	
6,966	-9,922	
6,621	-10,187	
3,340	-9,074	H_2O
3,296	-10,144	
3,110	-10,024	
3,072	-10,168	
2,505	-9,195	DMSO
2,071	-10,109	
1,595	-10,12	
1,536	-10,128	
1,314	-10,115	
0,000	-9,197	TMS

7 (1 mM, *T* = 300.1 K) protected bis-zwitterion

d [ppm]	log *D*	
12,350	-9,854	
11,851	-9,842	
8,560	-9,855	
7,761	-9,852	
7,386	-9,854	
6,824	-9,855	
6,772	-9,851	
5,289	-9,855	
3,499	-9,837	
3,322	-9,060	H_2O
3,047	-9,850	
2,502	-9,168	DMSO
2,039	-9,855	
1,482	-9,855	
1,273	-9,836	
0,000	-9,193	TMS

At high concentrations both monomer and dimer exist in solution. Because of this no clear signal assignment could be done for some of the CH_2 protons. For the calculation of the hydrodynamic radii r_H the diffusion coefficients *D* averaged over all observable non-exchanging nmr signals for each species were used.

$$r_H = \frac{k \cdot T}{6p \cdot h \cdot D}$$ (Stokes-Einstein equation)[3]

with:

$k = 1.38066 \cdot 10^{-23}$ N·m/K [3]

$?_{DMSO} = 1.987 \cdot 10^{-3}$ N·s/m^2 [4]

	Ø *D* [m^2/s]	$r_H \cdot 10^{-9}$ [m]
1 (1 mM)	$1{,}124 \cdot 10^{-10}$	0,98
1 (30 mM)	$7{,}759 \cdot 10^{-11}$	1,42
7 (1 mM)	$1{,}413 \cdot 10^{-10}$	0,78

[3] Elias, H.-G. *Polymere: Von Monomeren und Makromolekülen zu Werkstoffen* Hüthig & Wepf Verlag: Zug, Heidelberg, Oxford, CT/USA **1996**.

[4] Lide, D. R. *CRC Handbook of Chemistry and Physics 1995-1996, 76th Edition* CRC Press: Boca Raton, New York, London, Tokyo **1996**.

Atomic force microscopy

AFM investigations were performed under ambient conditions using a commercial scanning probe microscope operating in tapping mode. Silicon cantilevers with a resonance frequency of ~300 kHz were used. Samples of **1** were prepared by spin-coating of the respective solution (4 mM; dry DMSO) onto freshly cleaved mica at 10.000 rpm. Experiments were repeated the following two days with the same sample solution showing equivalent results. Statistical evaluation of the vesicle diameter and height was done by measuring the mean horizontal and vertical distance of 51 particles.

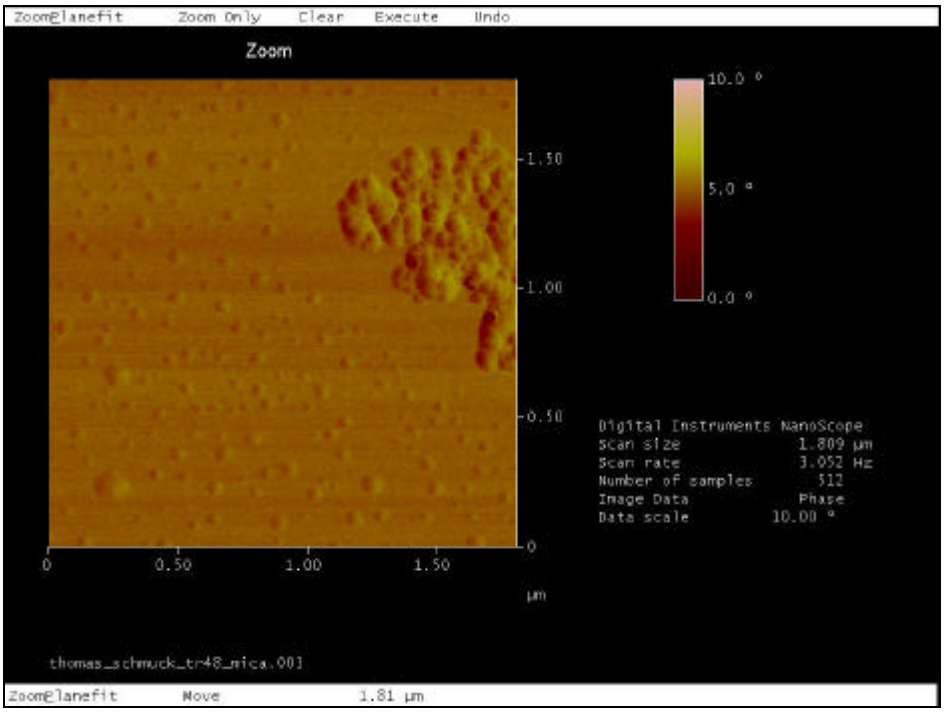

Figure S2. Overview of the vesicles of **1** and their larger aggregates.

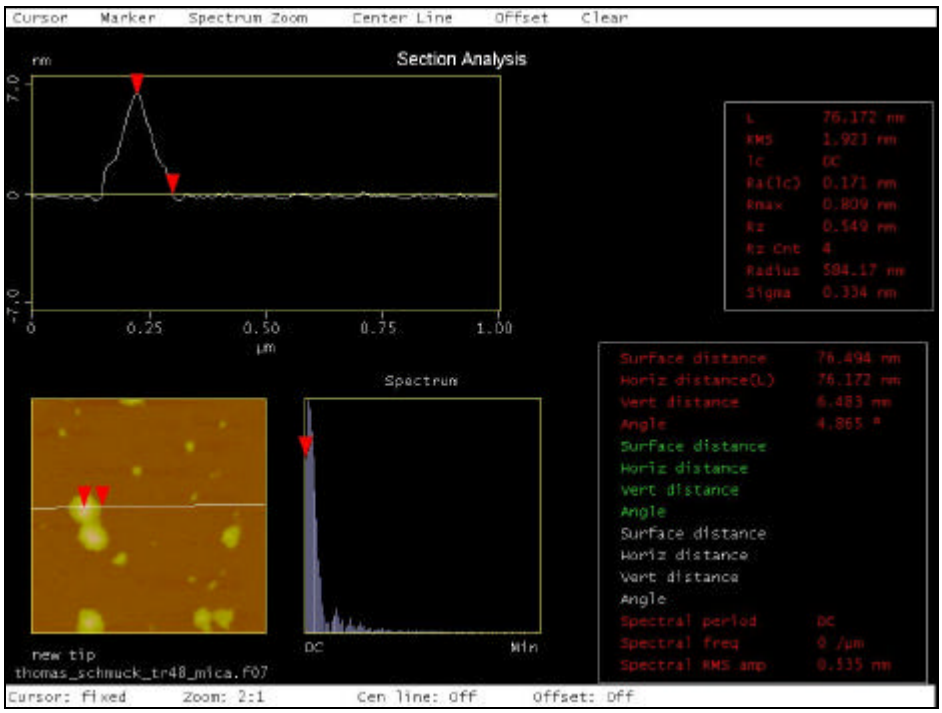

Figure S3. Contour plot of a distorted vesicle of **1** showing the shoulders that result from the interaction with the surface.

Molecular Modelling:

Molecular mechanics calculations were performed using the Macromodel V 8.0 software package. The implemented amber* force field was used with GB/SA water solvation treatment. In each case a Monte Carlo conformational search with at least 50.000 steps was performed. The resulting energy minimezd structures for the cyclic monomer, the cyclic dimer and a nonamer as a model for the vesicle structure are shown below.

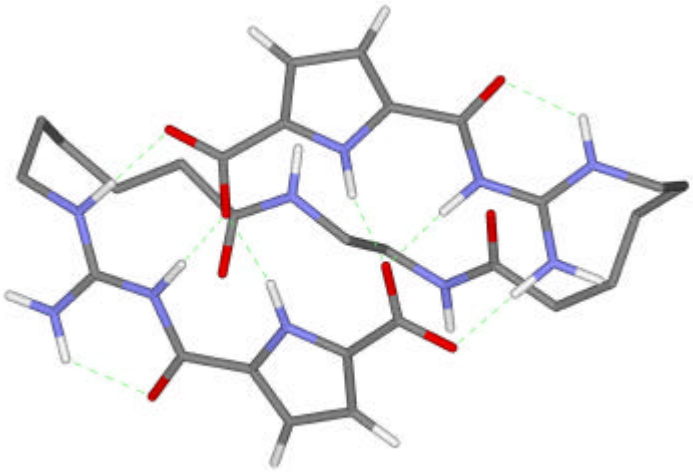

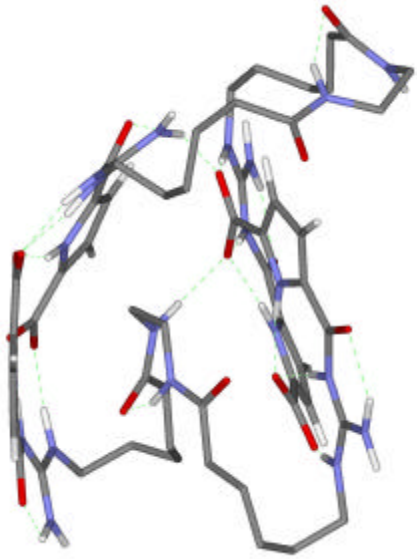

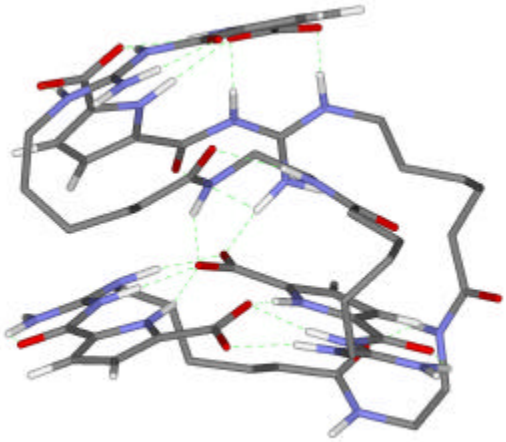

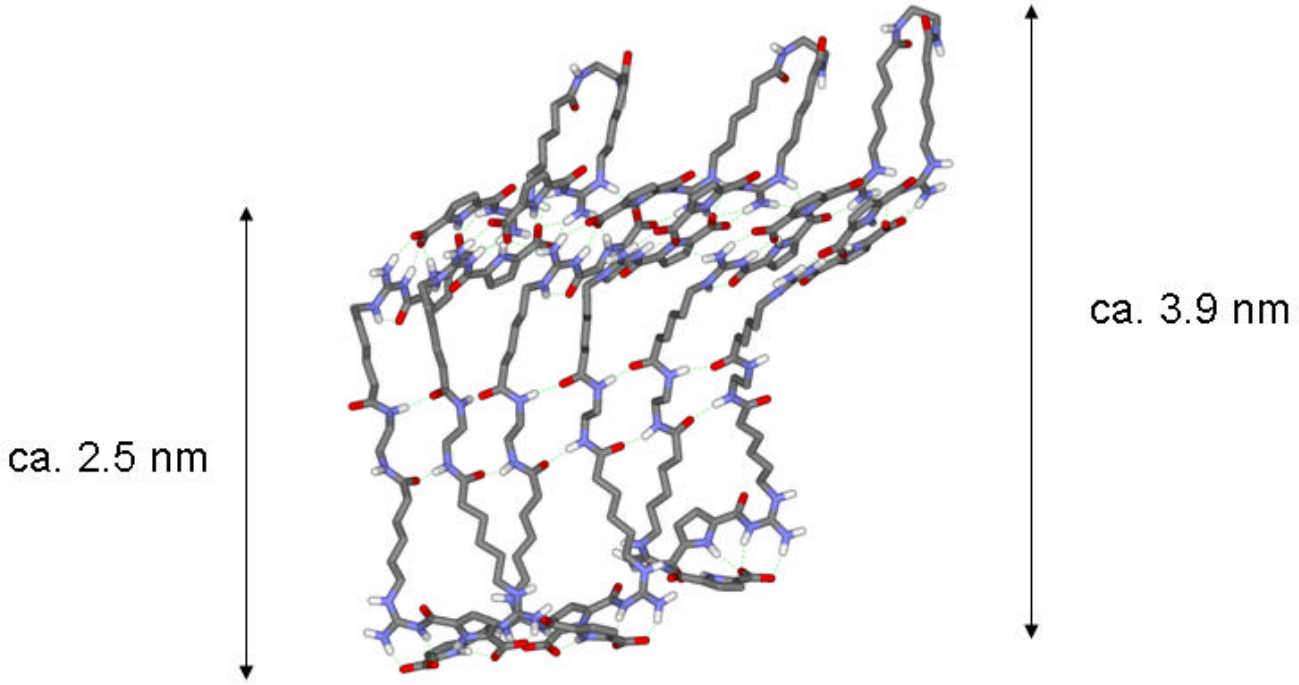

Figure S4. Calculated structures of **1** as a cyclic monomer (top), a cyclic dimer (middle) and a nonamer as a model for part of the vesicle wall (bottom). Hydrogen bonds are shown as dashed green lines, non-polar hydrogens are omitted for clarity.

Dynamic light scattering

Light scattering measurements were performed with a setup for combined static and dynamic light scattering consisting of an ALV/SP-86 goniometer and an ALV-5000/E multitau correlator. A He-Ne laser operating at a wavelength of 647.1 nm and a maximum output power of 100 mW was used as light source. A concentration range of 0.4 mM to 2 mM in DMSO was investigated. We compared measurements were the solutions were transferred by filtering through a Millipore 0.45 µm or 5 µm pore size teflon filter into 1 cm diameter dust free quartz cells and such without filtering prior to the measurement. Alternatively, solution we centrifuged between 700 and 15.000 rpm prior to the measurement. Measurements were performed at scattering angles of 30° to 150°. The volume corrected scattering intensity of the toluene standard lies within ± 2 % statistical error. The time autocorrelation function of the scattered intensity was measured (homodyne mode) and converted to the scattered electric field autocorrelation function via Siegert relation. The electric field autocorrelation function is analyzed via Inverse Laplace Transformation using the program CONTIN by S.Provencher.[5] The apparent diffusion coefficient was calculated from the inverse relaxation time and extrapolated to zero scattering vector square. The hydrodynamic radius cited in the manuscript is obtained via Stokes-Einstein relation from the averaged diffusion coefficients. The distribution as function of hydrodynamic radii rather than relaxation times or relaxation rates in Figure 2 is given for 90° scattering angle to demonstrate the size distribution more obviously.

Small angle neutron scattering (SANS)

Samples for SANS measurements were transferred into optical quality quartz cells with 2 mm path length. SANS studies were performed at the Institute Laue Langevin (ILL), Grenoble, France. Measurements were made using the D11 SANS instrument with a neutron wavelength λ = 0.6 nm and wavelength spread of $\Delta\lambda/\lambda$ = 0.11. Sample detector distances used were 26 m, 5.4 m and 1.2 m. A scattering vector range of 0.02 nm^{-1} to 3.2 nm^{-1} was covered. A concentration range of 2 mM to 15 mM in d-DMSO was investigated. Data were corrected for empty quartz cell scattering, electronic background and detector uniformity, and converted to an absolute scale using secondary standards. The data were further corrected by subtracting the contributions from solvent scattering and incoherent background.

After subtraction of incoherent background, the scattering curve I(q) is Fourier transformed into the three-dimensional averaged pair distance distribution function P(r) via the relationship

$$I(q) = 4\pi \int_{r=0}^{\infty} P(r) \frac{\sin(qr)}{qr} dr \qquad (1)$$

where r is the radial distance and q is the scattering wave vector magnitude. We apply the indirect transformation method in order to minimize termination effects. We use the program ITP, *Indirect transformation for the calculation of P(r),* by O. Glatter which includes smoothing of the primary data by a weighted least square procedure (estimation of the optimum stabilization parameter based on a stability plot), desmearing and transforming into real space simultaneously. The actual calculations dealing with the experimental scattering curves accounted for the measured beam profile and the wavelength distribution of the experimental setup.

Results show that the particles present are too large as compared to the measured q-range. This is in accordance with the fact, that the scattering curve itself still shows a slope at low q and the Guinier regime (of the complete particles) is not reached and the sizes observed in DLS.

However, once the geometry has been identified (via Thickness-Guinier Plot and AFM), alternative equations can be applied, e.g. for flat particles (or walls of large vesicles) the thickness pair distribution function $P_t(r)$ can be calculated via

$$\frac{q^2 I(q)}{2\pi A} = 2 \int_{r=0}^{\infty} P_t(r) \cos(qr) dr \qquad (2)$$

Transversal difference scattering-length-density profiles $\rho(x)$ are calculated from the thickness pair distance distribution function $P_t(r)$ by calculation of the convolution square root ("deconvoluting") using the program DECON (Glatter) which applies in the case of lamellae,

$$P_t(r) = 2 \int_{x=0}^{\infty} \rho_t(r) \rho_t(x - r) dx \qquad (3)$$

where $\rho_t(x)$ is the thickness scattering length density difference between the particle and the surrounding medium (sometimes notation $\Delta\rho_t(x)$). This deconvolution is possible in cases where interparticular contributions are negligible, and the experimental scattering function I(q) is identical with the particle form factor.

First, we allow a multiple step density profile. The resulting radial scattering length profile $\rho_t(x)$ is a multi-step profile of a decreasing density with increasing x. Second, we estimate how many actual steps are present in the density profile from this multiple step profile and the range in which they are located. Then we calculate the radial density profile again, under the assumption of one-step, two-step and three-step profiles, respectively. We look for the simplest solution that gives the best fit to $P_t(r)$. The result is shown in Figure 6 as the solid line. We find two pronounced steps in the thickness density profile: an inner core with a radius of 1.2 nm, plus an outer shell of 0.8 nm thickness. The total thickness d is 4 nm. The resolution in real space due to the sampling theorem is expected to be π/q_{max}, i.e. within the range of 1 nm. The fact that the P(r) function decays to zero at P(0) however indicates that there are no major resolution problems.

---

5 Provencher, S.W. *Comput. Phys. Commun.* **1982**, *27*, 229-242.